Supplement of Atmos. Chem. Phys., 26, 6611–6628, 2026
https://doi.org/10.5194/acp-26-6611-2026-supplement


Atmospheric Chemistry and Physics
Open Access
EGU

*Supplement of*

# Measurement report: Role of organic coating and chemical composition on ice nucleation potential of atmospheric particles in European Arctic

**Nurun Nahar Lata et al.**

*Correspondence to:* Naruki Hiranuma (smoon@utep.edu) and Swarup China (swarup.china@pnnl.gov)

# *Supplementary*

**S1. Micro-spectroscopy analysis**

Individual particles were classified based on their elemental composition (as atomic %) obtained from SEM-EDX measurements (**Figure S2**). Particles containing both phosphorus and potassium ≥ 0.4 at.% were identified as **biogenic**. The remaining **non-biogenic** particles were categorized into dust-laden, Na-laden, non-dust, and other groups. **Dust-laden particles** were defined by elevated mineral content ([Al, Si, Fe, Ca] ≥ 4 at.% and > [Na]) and were subdivided into **dust** ([C, N, O] < 85 at.%) and **aged dust** ([C, N, O] ≥ 85 at.%), the latter further classified as **carbonaceous-coated dust** ([S] < 1 at.%) or **sulfate-rich dust** ([S] ≥ 1 at.%). **Na-laden particles** were defined by [Na] > 1 at.% and [Na] ≥ [Al, Si, Fe, Ca], and were classified as **Na-rich** when [Na] ≥ [S] or as **Na-rich sulfates** when [Na] < [S]. Among **non-dust particles** ([Al, Si, Fe, Ca] < 4 at.%), those dominated by [C, N, O, S] (> 99 at.%) with [S] ≥ 0.5 at.% were classified as **sulfates**, while those dominated by [C, N, O] (> 99 at.%) were classified as **carbonaceous**. Particles that did not meet any of the above criteria were grouped as **other**.

**S2. Surface Type Influence and Free-Tropospheric Residence from FLEXPART Back-Trajectories**

We used FLEXPART back-trajectory analysis to estimate the surface type influence and free-tropospheric (FT) residence time for ground-level aerosol samples (SA1–SA5) over a 168-hour period. The calculated percentages represent the time air masses spent over closed ice, open ice, open water, and land, as well as the duration spent in the FT, based on ERA5 reanalysis data and back-trajectory altitudes relative to the boundary layer (**Table S3**). Additionally, black carbon contributions were inferred from source apportionment using ERA5 sea ice edge data combined with back-trajectory analysis (**Figure S3 and Table S4**). These metrics provide critical context for understanding the origin, transport pathways, and potential ageing processes of sampled aerosols, which are important for interpreting their observed ice-nucleating properties.

**S3. Sea-ice edge data**

Sea-ice edge/coverage shown in Figure S4 was taken from the Copernicus Climate Data Store (CDS) "Sea ice edge and type daily gridded data from 1978 to present" product (DOI: 10.24381/cds.29c46d83; accessed January 2026). The dataset is derived from satellite passive-microwave brightness temperatures and provided at daily (24 h) temporal resolution on a 12.5 km grid. Each grid cell is classified into open water, open ice, or closed ice based on the sea-ice amount, and we used the field corresponding to the first sampling day for each sample to provide consistent sea-ice context across cases (Copernicus Climate Change Service (C3S), 2020).

**S4. INP concentration calculation:**

First, the concentration of ice-nucleating particles in the HPLC suspension, $C_{\mathrm{INP}}(T)$($\mathrm{L}^{-1}$) was calculated from the droplet-freezing assay as-

$$C_{INp}(T) = -\frac{\ln\left(f_{unfrozen}(T)\right)}{V_d} \qquad [1]$$

where $f_{\mathrm{unfrozen}}$ is the fraction of droplets that remained unfrozen at temperature $T$(i.e., the number of unfrozen droplets divided by the total number of droplets), and $V_d$is the volume of an individual droplet ($V_d = 3$ µL).

Next, ambient INP concentrations, $n_{\mathrm{INP}}(T)$($L^{-1}$ air), were obtained by scaling $C_{\mathrm{INP}}(T)$using the dilution applied during analysis and the ratio of suspension volume to sampled air volume:

$$n_{INP}(T) = C_{INP}(T) \times DF \times \frac{V_1}{V_{air}} \quad [2]$$

where $DF$is the serial dilution factor (e.g., 1, 10, 100, …), $V_{\mathrm{air}}$is the sampled air volume, and $V_1$is the (provided) total volume of the original suspension associated with the analyzed sample.

**S5. Fraction of heat labile and heat stable INP calculation:**

Equations 1 and 2 show the calculation of heat labile and stable INP percentages, respectively.

$$\%INP_{Heat\ Labile}(T) = \frac{n_{INP,untreated}(T) - n_{INP,heated}(T)}{n_{INP,untreated}(T)} \times 100 \quad [3]$$

$$\%INP_{Heat\ Stable}(T) = 100 - \%INP_{Heat\ Labile}(T) \quad [4]$$

where $n_{INP,untreated}$ (T) is the number concentration of INPs before heat treatment and $n_{INP,heated}(T)$ is the number concentration of INPs after heat treatment at that temperature.

INP concentrations and their differences span orders of magnitude and are commonly interpreted on a logarithmic scale. The heat-labile fraction reported here is calculated as a linear percent difference between paired $n_{INP}$(T) spectra (Eqs. 3-4) and should therefore be interpreted as an approximate and comparative metric. In particular, when $n_{INP}$, heated (T) approaches the detection limit, the inferred fraction becomes sensitive to detection-limit treatment. We use this metric to summarize relative heat sensitivity across samples rather than to define an absolute biological fraction.

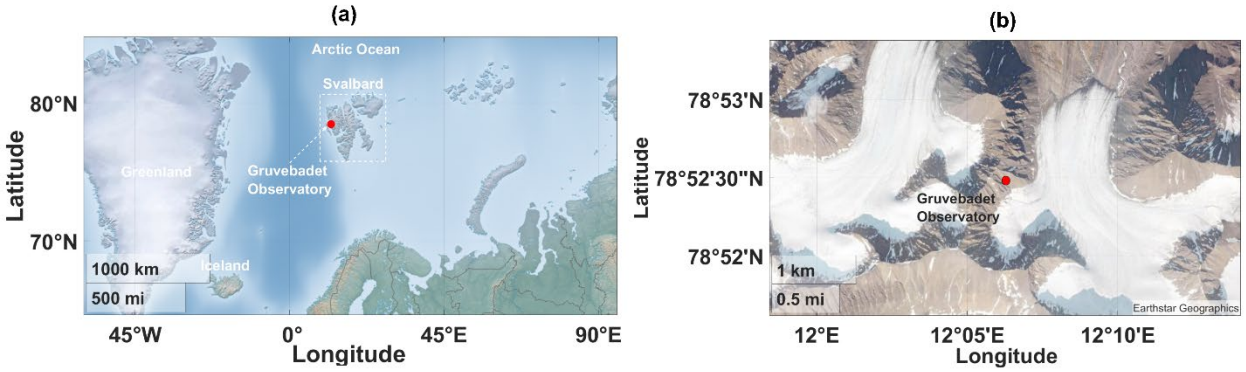


**Figure S1.** Location of the Gruvebadet Observatory in Ny-Ålesund, Svalbard (red dot), situated in the European Arctic. (a) The regional map highlights the surrounding regions, including Greenland, Iceland, and the Arctic Ocean, with a focus on the observatory's proximity to marine and polar environments; the white dashed box outlines the Svalbard archipelago. (b) Zoomed-in view of the Svalbard archipelago showing the Gruvebadet Observatory location in detail. Scale bars represent distances in kilometers and miles. Map generated in MATLAB (R2024b) using a KML file downloaded from Google Earth (earth.google.com) Map data © 2024 Google. The shaded-relief basemap is Esri, Maxar, Earthstar Geographics, and the GIS User Community | Powered by Esri.

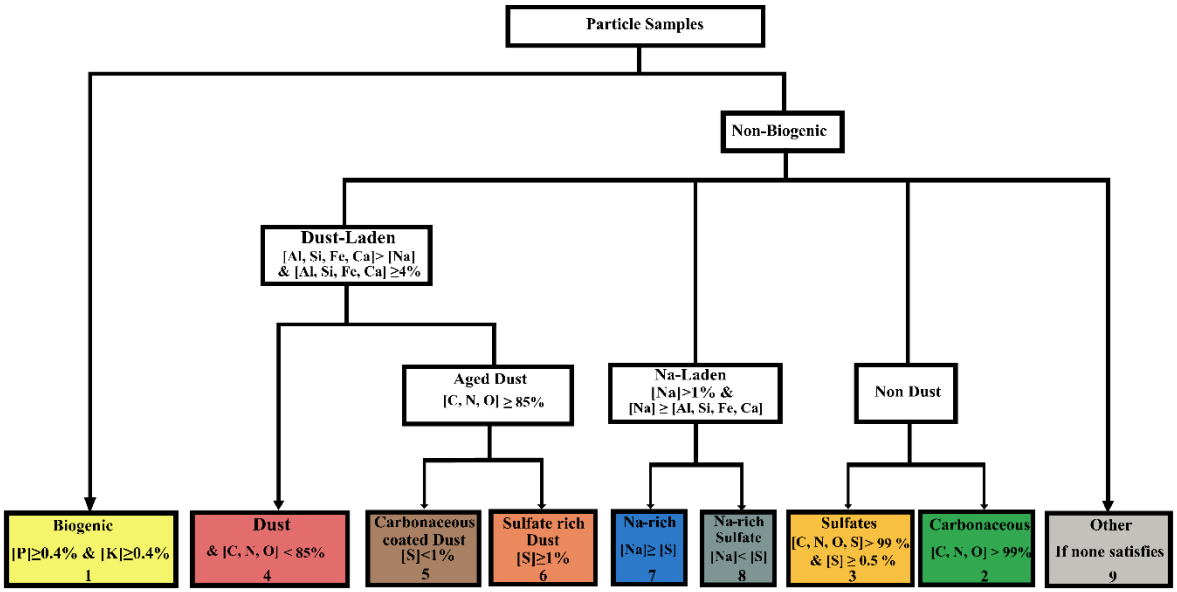


**Figure S2.** Particle classification scheme based on elemental composition from SEM-EDX analysis. Particles are first categorized as biogenic or non-biogenic. Non-biogenic particles are further classified into dust-laden, Na-laden, non-dust, and other types, with each main group subdivided based on dominant elemental composition and sulfur content.

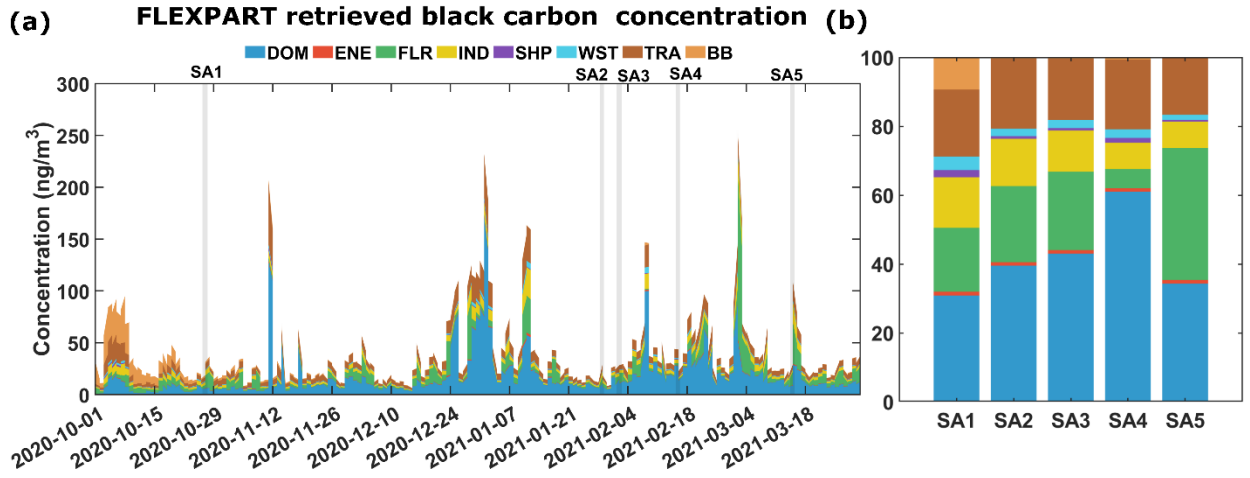


**Figure S3.** (a) Temporal variation of black carbon (BC) concentration (ng/m³) for ground-level aerosol samples (SA1–SA5) from October 2020 to March 2021. The BC source contributions are categorized as domestic emissions (**DOM**, blue), energy production (**ENE**, red), flaring (**FLR**, green), industrial activities (**IND**, yellow), shipping (**SHP**, purple), waste burning (**WST**, pink), transportation (**TRA**, brown), and biomass burning (**BB**, orange). Sampling events (SA1–SA5) are marked with grey bands.
(b) Relative contribution (%) of BC sources to total BC concentration for each sample (SA1–SA5), highlighting variability across different sampling periods.

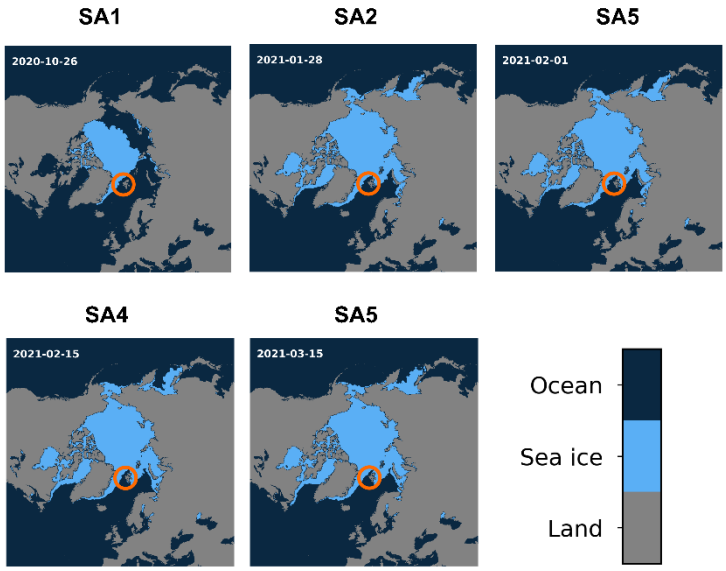


**Figure S4:** Sea-ice edge during sampling. Maps show sea-ice coverage on the first day of each sampling period (SA1–SA5). Light blue denotes sea ice, dark blue denotes open ocean, and gray denotes land. The red circle marks the sampling location at Gruvebadet Laboratory (GAL), Ny-Ålesund, Svalbard.

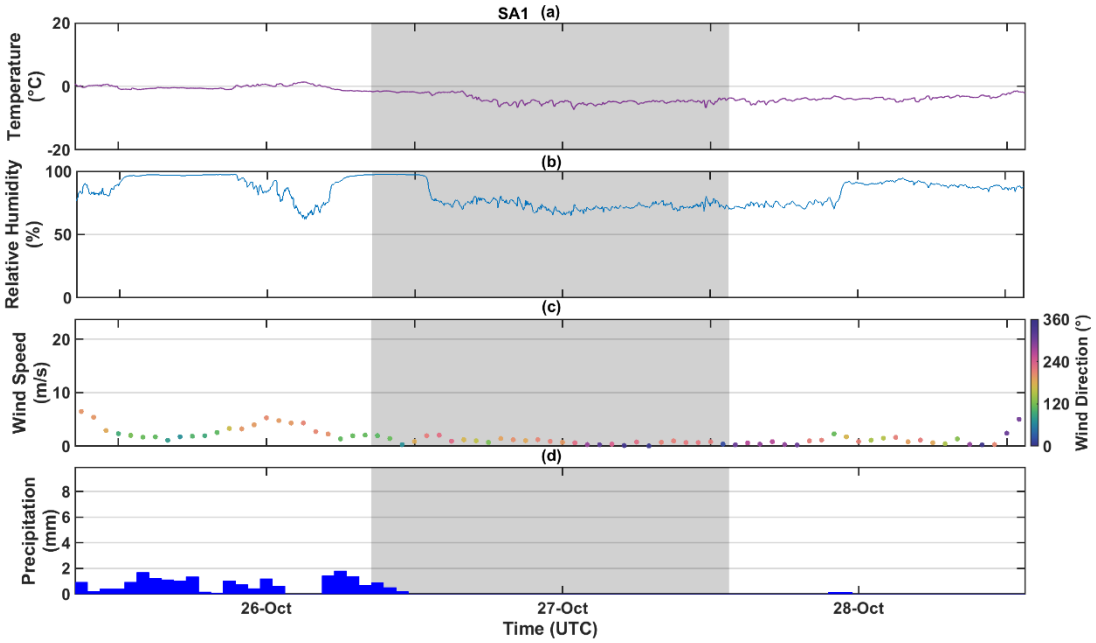


**Figure S5.** Zoomed-in hourly meteorological parameters for SA1 as indicated by the shaded regions in Figure 1. Panels represent (a) Temperature (°C), (b) Relative Humidity (%), (c) Wind Speed (m $s^{-1}$) with color-coded Wind Direction (°), and (d) Precipitation (mm). The expanded time axis for each subplot allows for a detailed assessment of local meteorological conditions and potential atmospheric processing during the individual filter collection periods.

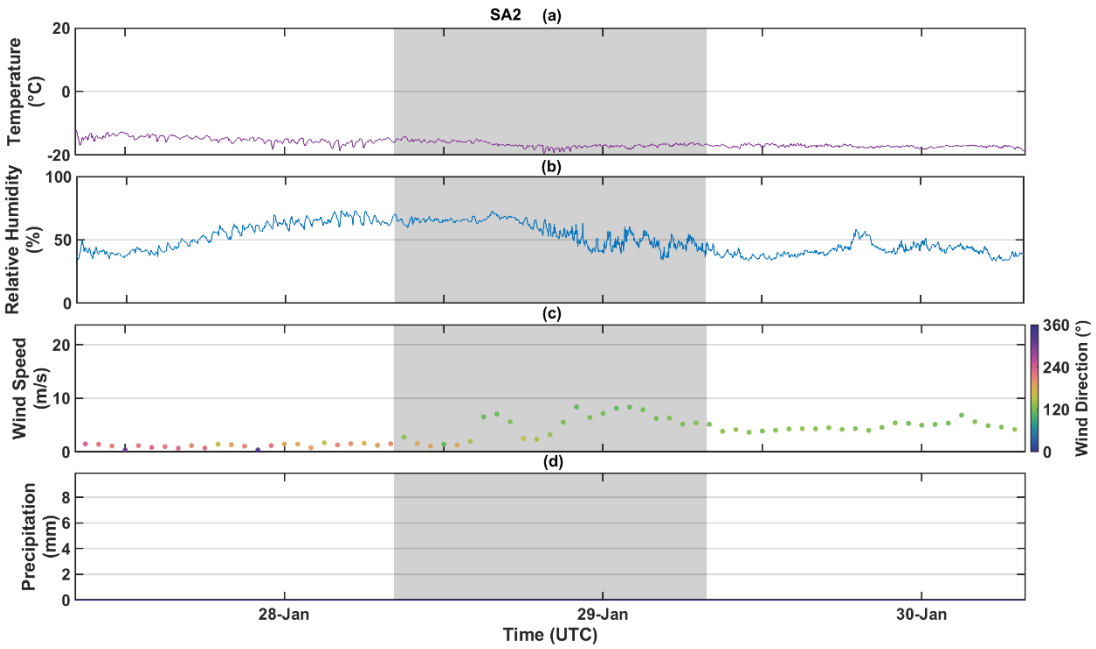


**Figure S6.** Zoomed-in hourly meteorological parameters for SA2 as indicated by the shaded regions in Figure 1. Panels represent (a) Temperature (°C), (b) Relative Humidity (%), (c) Wind Speed (m $s^{-1}$) with color-coded Wind Direction (°), and (d) Precipitation (mm). The expanded time axis for each subplot allows for a detailed assessment of local meteorological conditions and potential atmospheric processing during the individual filter collection periods.

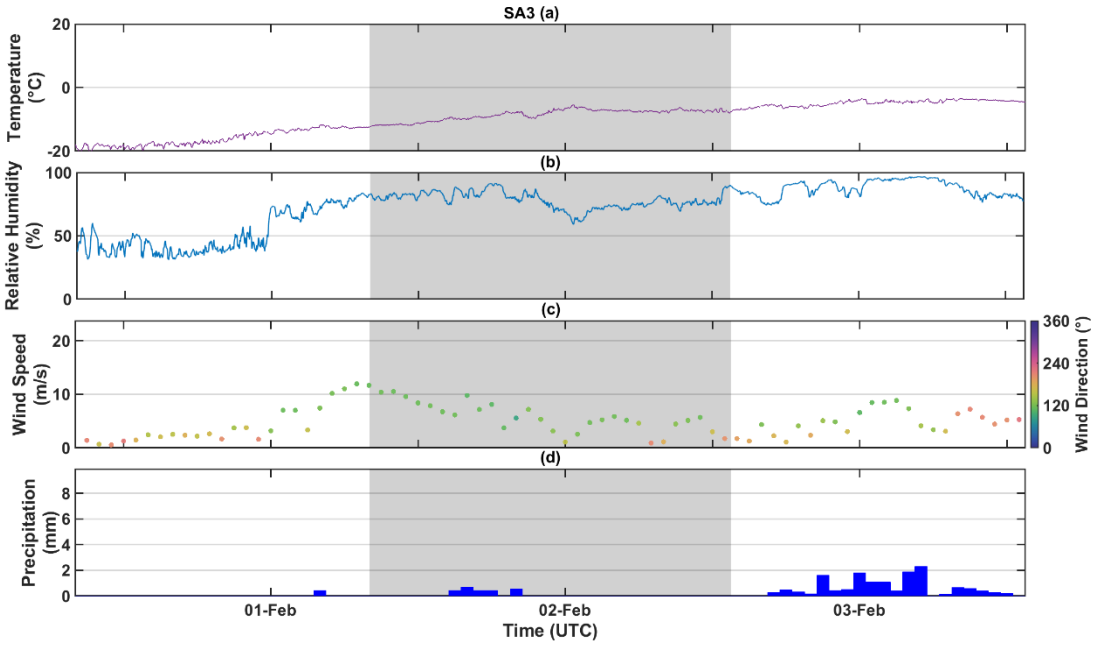


**Figure S7.** Zoomed-in hourly meteorological parameters for S3 as indicated by the shaded regions in Figure 1. Panels represent (a) Temperature (°C), (b) Relative Humidity (%), (c) Wind Speed (m $s^{-1}$) with color-coded Wind Direction (°), and (d) Precipitation (mm). The expanded time axis for each subplot allows for a detailed assessment of local meteorological conditions and potential atmospheric processing during the individual filter collection periods.

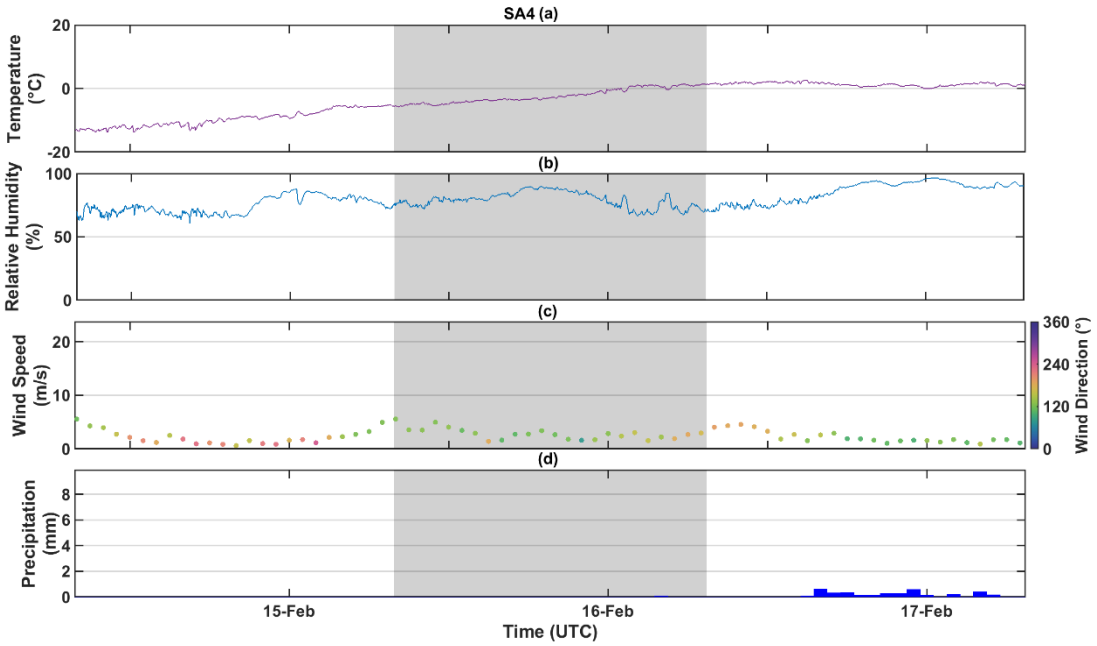


**Figure S8.** Zoomed-in hourly meteorological parameters for SA4 as indicated by the shaded regions in Figure 1. Panels represent (a) Temperature (°C), (b) Relative Humidity (%), (c) Wind Speed (m $s^{-1}$) with color-coded Wind Direction (°), and (d) Precipitation (mm). The expanded time axis for each subplot allows for a detailed assessment of local meteorological conditions and potential atmospheric processing during the individual filter collection periods.

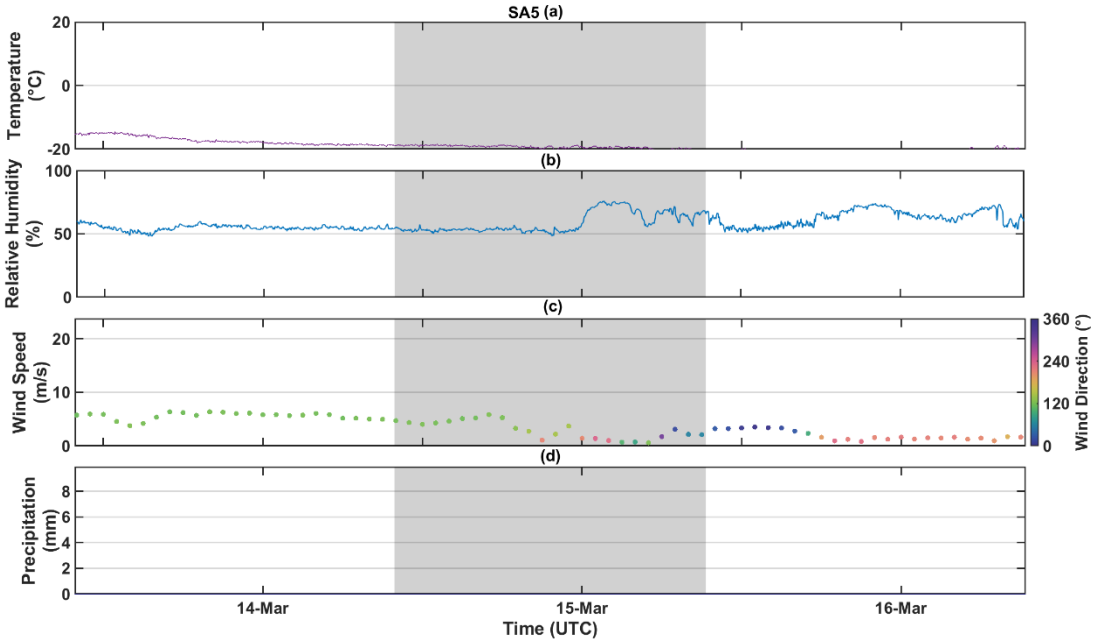


**Figure S9.** Zoomed-in hourly meteorological parameters for SA5 as indicated by the shaded regions in Figure 1. Panels represent (a) Temperature (°C), (b) Relative Humidity (%), (c) Wind Speed (m $s^{-1}$) with color-coded Wind Direction (°), and (d) Precipitation (mm). The expanded time axis for each subplot allows for a detailed assessment of local meteorological conditions and potential atmospheric processing during the individual filter collection periods.

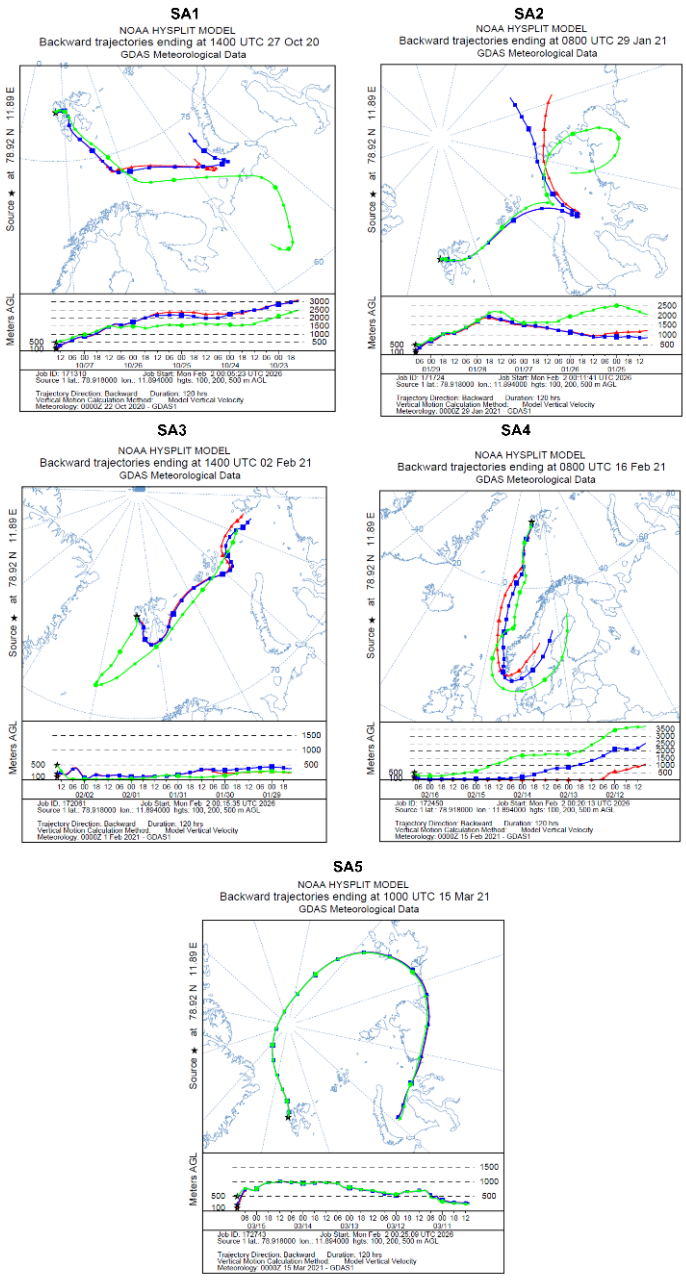


**Figure S10**. Height-resolved 120 h NOAA HYSPLIT backward trajectories for the five sampling periods (SA1–SA5), driven by GDAS meteorological fields. For each sample, trajectories are shown for endpoints at 100 m (red), 200 m (blue), and 500 m (green) above ground level (AGL) at the sampling location (star). The lower panels show the corresponding altitude history along each trajectory. This sensitivity analysis illustrates that the inferred transport pathways and source regions are broadly consistent across the selected endpoint heights.

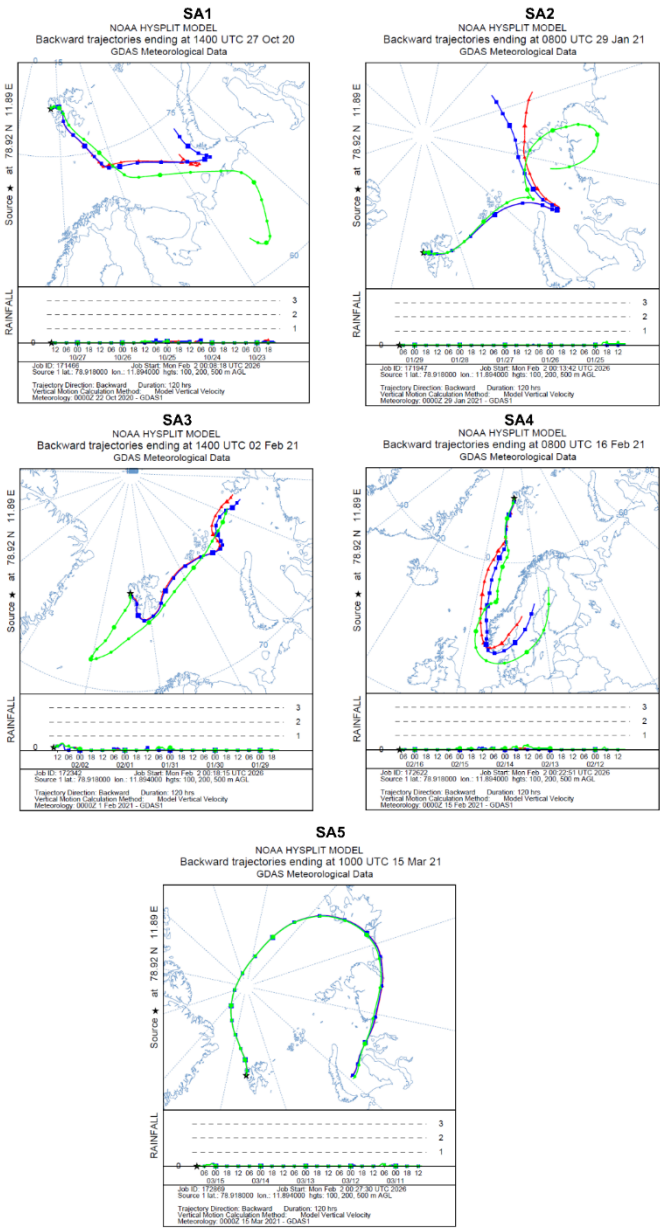


**Figure S11.** Backward air-mass trajectories and precipitation along transport pathways. NOAA HYSPLIT 120 h backward trajectories for samples SA1–SA5 (ending at the sampling site; star). Colored lines indicate trajectories initialized at 100, 200, and 500 m AGL. The lower panel in each plot shows the accumulated precipitation (rainfall) along each trajectory as reported by HYSPLIT, used to assess potential wet removal prior to arrival at the measurement site.

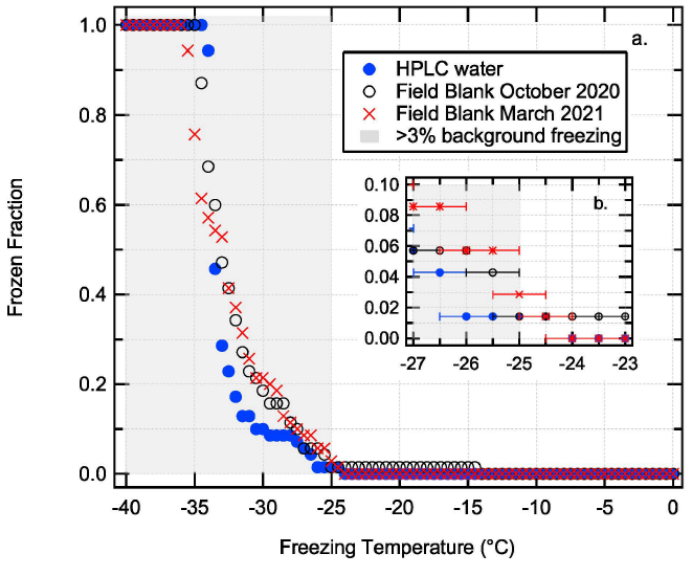


**Figure S12**. Frozen fraction of HPLC water, as well as field blanks suspended in 5 mL of HPLC water, as a function of freezing temperature. Two field blanks were collected prior to sampling SA1-INP and after sampling SA5-INP. Panel (b) represents a magnified frozen fraction spectra with a temperature uncertainty of ±0.5 °C.

**Table S1.** Summary of meteorological parameters during the sampling periods (SA1–SA5). Each value represents the mean ± standard deviation for air temperature (°C), relative humidity (%), wind speed (m/s) and precipitation (mm) within the specified intervals of sampling time.

| Samples | Mean temperature (°C) | Mean RH (%) | Mean wind speed (m/s) | Mean precipitation (mm) |
|---|---|---|---|---|
| SA1 | -4.1 ± 1.5 | 76.9 ± 9.3 | 0.9 ± 0.7 | 0.05 ± 0.19 |
| SA2 | -16.7 ± 0.9 | 56.7 ± 9.7 | 4.8 ± 2.9 | 0.00 ± 0.00 |
| SA3 | -8.6 ± 1.7 | 78.2 ± 6.5 | 5.8 ± 3.1 | 0.09 ± 0.20 |
| SA4 | -2.3 ± 2.2 | 79.3 ± 6.2 | 2.8 ± 1.5 | 0.00 ± 0.02 |
| SA5 | -19.4 ± 0.6 | 58.9 ± 8.0 | 3.0 ± 1.9 | 0.00 ± 0.00 |

**Table S2.** Summary of offline chemical analysis (CCSEM/EDX and STXM/NEXAFS) of the samples (SA1–SA5). Each value represents the number percentage ± standard deviation.

| Offline chemical analysis | Type of analysis | Classes | SA1 | SA2 | SA3 | SA4 | SA5 |
|---|---|---|---|---|---|---|---|
| CCSEM/EDX | Particle classes (# percentage) | Biogenic | 3.9 ± 0.3 | 0.9 ± 0.1 | 0.0 ± 0.0 | 6.1 ± 0.6 | 12.8 ± 1.0 |
| | | Carbonaceous | 11.2 ± 0.5 | 4.6 ± 0.3 | 18.7 ± 1.3 | 19.7 ± 1.0 | 13.3 ± 1.0 |
| | | Sulfate | 5.3 ± 0.4 | 5.6 ± 0.3 | 32.1± 1.5 | 18.4 ± 0.9 | 1.7 ± 0.4 |
| | | Dust | 0.8 ± 0.1 | 3.0 ± 0.3 | 1.2 ± 0.4 | 1.0 ± 0.2 | 1.7± 0.4 |
| | | Carbonaceous+Dust | 0.2 ± 0.1 | 0.1 ± 0.0 | 0.3 ± 0.2 | 0.1 ± 0.1 | 0.0 ± 0.0 |
| | | Sulfate+Dust | 0.1 ± 0.1 | 0.4± 0.1 | 0.4 ± 0.2 | 0.1 ± 0.1 | 0.0 ± 0.0 |
| | | Na-rich | 70.3 ± 0.7 | 69.0 ± 0.7 | 22.9 ± 1.4 | 39.8 ± 1.2 | 66.2 ± 1.4 |
| | | Na-rich Sulfate | 4.5 ± 0.3 | 8.3 ± 0.4 | 20.2 ± 1.3 | 5.2 ± 0.5 | 1.2 ± 0.3 |
| | | Other | 3.8 ± 0.3 | 8.1 ± 0.4 | 4.2 ± 0.6 | 9.6 ± 0.7 | 3.1 ± 0.5 |
| STXM/NEXAFS | Mixing state classes (# percentage) | In | 2.2 ± 0.9 | 0.4 ± 0.4 | 3.3 ± 0.8 | 3.9 ± 0.9 | 0.0 ± 0.0 |
| | | OC | 12.9 ± 2.0 | 16.1 ± 2.3 | 22.5 ± 1.8 | 12.0 ± 1.5 | 5.7 ± 1.1 |
| | | OCEC | 4.1 ± 1.2 | 2.7 ± 1.0 | 4.8 ± 0.9 | 1.0 ± 0.5 | 0.7 ± 0.4 |
| | | OCIn | 52.4 ± 3.0 | 73.6 ± 2.7 | 44.7 ± 2.2 | 77.1 ± 1.9 | 85.0 ± 1.7 |
| | | OCInEC | 28.4 ± 2.7 | 7.3 ± 1.6 | 24.7 ± 1.9 | 6.0 ± 1.1 | 8.6 ± 1.4 |
| | OVF classes (# percentage) | <20% | 36.5 ± 2.9 | 8.4 ± 1.7 | 16.4 ± 1.6 | 33.2 ± 2.1 | 19.3 ± 1.9 |
| | | 20-40% | 17.0 ± 2.3 | 25.3 ± 2.7 | 43.0 ± 2.2 | 43.3 ± 2.2 | 31.4 ± 2.3 |
| | | 40-60% | 20.7 ± 2.5 | 30.7 ± 2.9 | 30.3 ± 2.0 | 18.1 ± 1.7 | 26.7 ± 2.2 |
| | | 60-80% | 12.5 ± 2.0 | 27.2 ± 2.8 | 9.2 ± 1.3 | 4.3 ± 0.9 | 16.2 ± 1.8 |
| | | 80-100% | 13.3 ± 2.1 | 8.4 ± 1.7 | 1.2 ± 0.5 | 1.0 ± 0.5 | 6.4 ± 1.2 |
| | | Overall OVF (mean) | 0.4 ± 0.3 | 0.5 ± 0.2 | 0.4± 0.2 | 0.3 ± 0.2 | 0.4± 0.2 |
| | | Overall OVF (median [Q1–Q3]) | 0.4 [0.1–0.6] | 0.5 [0.3–0.7] | 0.4 [0.3–0.5] | 0.3 [0.2–0.4] | 0.4 [0.2–0.6] |

**Table S3.** Surface type influence and free tropospheric (FT) residence time for ground-level aerosol samples (SA1–SA5) over a 168-hour back-trajectory period obtained from Flexpart. Percentages represent the time spent over closed ice, open ice, open water, land, and within the free troposphere (FT), calculated using ERA5 reanalysis data and back-trajectory altitudes relative to the boundary layer.

| Sample | Time over closed ice (168h) | Time over open ice (168h) | Time over open water (168h) | Time over land (168h) | Time in FT (168h) |
|---|---|---|---|---|---|
| | % | % | % | % | % |
| **SA1** | 1.72 | 0.12 | 1.36 | 8.88 | 87.93 |
| **SA2** | 11.39 | 1.33 | 0.37 | 6.07 | 80.84 |
| **SA3** | 9.29 | 0.95 | 2.78 | 8.52 | 78.46 |
| **SA4** | 2.51 | 1.85 | 11.02 | 1.33 | 83.28 |
| **SA5** | 40.31 | 0.15 | 1.78 | 17.90 | 39.87 |

**Table S4**. Black carbon (BC) source contributions for ground-level aerosol samples (SA1–SA5). BC sources include domestic emissions (BC_DOM), energy production (BC_ENE), flaring (BC_FLR), industrial activities (BC_IND), shipping emissions (BC_SHP), waste burning (BC_WST), transportation (BC_TRA), and biomass burning (BC_BB). Percentages were derived using sea ice edge data from ERA5 reanalysis and back-trajectory altitude relative to the boundary layer.

| Sample | BC_DOM | BC_ENE | BC_FLR | BC_IND | BC_SHP | BC_WST | BC_TRA | BC_BB |
|---|---|---|---|---|---|---|---|---|
| | % | % | % | % | % | % | % | % |
| **SA1** | 30.86 | 1.10 | 18.56 | 14.66 | 2.09 | 3.95 | 19.44 | 9.34 |
| **SA2** | 39.54 | 1.00 | 22.08 | 13.74 | 0.78 | 2.17 | 20.36 | 0.33 |
| **SA3** | 43.03 | 1.03 | 22.78 | 11.92 | 0.71 | 2.41 | 17.77 | 0.36 |
| **SA4** | 61.02 | 0.99 | 5.58 | 7.64 | 1.39 | 2.51 | 20.24 | 0.63 |
| **SA5** | 34.26 | 1.12 | 38.35 | 7.67 | 0.51 | 1.44 | 16.50 | 0.14 |

**Table S5.** Ice nucleating particle (INP) concentrations for ground-level aerosol samples (SA1–SA5) under untreated and heat-treated conditions. INP concentrations (# of INP/L) were measured across temperatures ranging from –7.5°C to –25 °C to evaluate the effect of heat treatment n INP activity.

| Temperature (°C) | SA1 (# of INP/L) | SA1_heat treated (# of INP/L) | SA2_ (# of INP/L) | SA2_heat treated (# of INP/L) | SA3 (# of INP/L) | SA3_heat treated (# of INP/L) | SA4 (# of INP/L) | SA4_heat treated (# of INP/L) | SA5 (# of INP/L) | SA5_heat treated (# of INP/L) |
|---|---|---|---|---|---|---|---|---|---|---|
| -7.500 | - | - | - | - | 0.001 | - | - | - | - | - |
| -8.000 | - | - | - | - | 0.001 | - | - | - | - | - |
| -8.500 | - | - | - | - | 0.001 | - | - | - | - | - |
| -9.000 | - | - | - | - | 0.001 | - | - | - | - | - |
| -9.500 | - | - | - | - | 0.001 | - | - | - | - | - |
| -10.000 | - | - | 0.001 | - | 0.001 | - | - | - | 0.001 | - |
| -10.500 | - | - | 0.001 | - | 0.001 | - | - | - | 0.001 | - |
| -11.000 | - | - | 0.001 | - | 0.001 | - | - | - | 0.001 | - |
| -11.500 | - | - | 0.001 | - | 0.002 | - | - | - | 0.001 | - |
| -12.000 | - | - | 0.001 | - | 0.002 | - | - | - | 0.001 | - |
| -12.500 | - | - | 0.001 | - | 0.002 | - | - | - | 0.001 | - |
| -13.000 | - | - | 0.002 | - | 0.002 | - | - | - | 0.001 | - |
| -13.500 | 0.001 | 0.001 | 0.002 | - | 0.002 | - | - | - | 0.002 | - |
| -14.000 | 0.002 | 0.001 | 0.002 | - | 0.002 | - | 0.001 | - | 0.003 | - |
| -14.500 | 0.002 | 0.001 | 0.002 | - | 0.003 | - | 0.001 | - | 0.003 | - |
| -15.000 | 0.004 | 0.001 | 0.002 | - | 0.003 | - | 0.001 | - | 0.003 | - |
| -15.500 | 0.004 | 0.001 | 0.002 | - | 0.003 | - | 0.001 | - | 0.003 | - |
| -16.000 | 0.004 | 0.001 | 0.002 | - | 0.003 | - | 0.001 | - | 0.003 | - |
| -16.500 | 0.005 | 0.001 | 0.003 | - | 0.003 | - | 0.001 | - | 0.003 | - |
| -17.000 | 0.005 | 0.001 | 0.003 | - | 0.003 | - | 0.002 | - | 0.003 | - |
| -17.500 | 0.006 | 0.001 | 0.005 | - | 0.003 | - | 0.002 | - | 0.003 | - |
| -18.000 | 0.007 | 0.001 | 0.007 | - | 0.003 | - | 0.003 | - | 0.003 | - |
| -18.500 | 0.008 | 0.001 | 0.007 | - | 0.006 | - | 0.003 | - | 0.005 | - |
| -19.000 | 0.010 | 0.001 | 0.010 | - | 0.008 | - | 0.003 | - | 0.011 | - |
| -19.500 | 0.011 | 0.002 | 0.011 | 0.001 | 0.011 | 0.001 | 0.003 | - | 0.013 | 0.001 |
| -20.000 | 0.013 | 0.003 | 0.013 | 0.002 | 0.014 | 0.003 | 0.004 | - | 0.023 | 0.004 |
| -20.500 | 0.017 | 0.003 | 0.018 | 0.005 | 0.017 | 0.005 | 0.004 | - | 0.034 | 0.012 |
| -21.000 | 0.022 | 0.004 | 0.026 | 0.005 | 0.023 | 0.013 | 0.005 | 0.002 | 0.042 | 0.036 |
| -21.500 | 0.029 | 0.006 | 0.039 | 0.010 | 0.031 | 0.021 | 0.010 | 0.003 | 0.052 | 0.080 |
| -22.000 | 0.039 | 0.006 | 0.057 | 0.018 | 0.032 | 0.032 | 0.018 | 0.003 | 0.074 | 0.135 |
| -22.500 | 0.048 | 0.012 | 0.077 | 0.023 | 0.039 | 0.059 | 0.029 | 0.004 | 0.087 | 0.183 |
| -23.000 | 0.080 | 0.014 | 0.107 | 0.028 | 0.071 | 0.087 | 0.050 | 0.011 | 0.112 | 0.247 |
| -23.500 | 0.117 | 0.019 | 0.151 | 0.036 | 0.094 | 0.107 | 0.091 | 0.014 | 0.135 | 0.247 |
| -24.000 | 0.199 | 0.032 | 0.219 | 0.050 | 0.117 | 0.112 | 0.107 | 0.014 | 0.219 | 0.295 |
| -24.500 | 0.295 | 0.042 | 0.295 | 0.098 | 0.171 | 0.142 | 0.129 | 0.021 | 0.247 | - |
| -25.000 | 0.295 | 0.052 | 0.339 | 0.135 | 0.219 | 0.199 | 0.199 | 0.023 | 0.295 | - |